

Productivity Simulation of Gas and Water Flow in Fractured Tight Gas Reservoir

Liqiang Zhao^{1,a}, Lin Wu^{1,*}

¹State Key Laboratory of Oil and Gas Reservoir Geology and Exploitation, Southwest Petroleum University, Chengdu 610500, China.

^azhaolq@vip.163.com, *sgywlin@163.com

Abstract

Based on the equivalent permeability tensor model of fractured medium, a numerical model, considering of stress sensitivity, slippage effect, permeability anisotropy, for gas-water two phases flowing in fractured gas reservoirs was established. Also the equation of gas production was established, based on the generalized Darcy formula and the law of conservation of mass. The effect of various factors on gas production was analyzed with examples. The results of case analysis show that: The stress sensitivity, slippage effect, and non Darcy flow can not be ignored in calculating the production of fractured reservoir gas wells; The greatest factor that causes the production drawdown is stress sensitivity; In the early stage of production, the formation energy is sufficient, and the influence of stress sensitivity is relatively small. With the decrease of formation energy, the stress sensitivity is more and more obvious when natural fractures are closed. In the later stage of production, the width and permeability of natural fractures tend to be fixed, and the stress sensitivity gradually weakens; The more natural fractures, the more obvious decrease of production occurred by stress sensitivity; Lower production pressure helps to weaken the stress sensitivity effect and prolong the life of the gas well.

Keywords

Natural fractures; Stress sensitivity; Slippage effect; Non Darcy flow; Equivalent permeability tensor.

1. Introduction

Natural fracture is the main seepage channel in fractured tight gas reservoir, and its nature plays a key role in gas well productivity. With the continuous production of gas, formation pressure decreases, plastic deformation of reservoir rock occurs and natural fractures close, showing stress-sensitive characteristics[1-4]. In addition, when the average free path of gas molecule is not negligible relative to the pore size, the diffusion of gas molecule can move freely without collision, and there is no adsorptive thin layer on the pore wall. There is no significant difference in the flow velocity between the pore center and the pore wall, resulting in an increase in apparent permeability[5-6]. For gas-water co-production wells, water saturation increases gradually and gas permeability decreases during production. If the decrease of gas permeability caused by water saturation is not taken into account, the gas well productivity will be higher[7-9].

There are many research results on stress sensitivity, slippage effect and the effects of water saturation on permeability at home and abroad. Yu-Long Zhao[10] established a non-linear fluid flow mathematical model considering stress sensitivity, assuming that the permeability was exponentially related to the pressure of the fracture system, and solved it in Laplace space by using perturbation theory, Laplace and Fourier transform. Yongfei Yang[11] used an experimental method to identify the real pore space characteristics of core samples by CT scanning, and combined with digital core and pore network model, established the relationship between pore structure and effective stress. Arash Behrang[12] derived the calculation formula of effective mass diffusion coefficient in porous media by using the analogy of gas dynamics theory and heat and mass transfer and calculated absolute permeability based on Kozeny-Carman equation and fractal theory. Eric Aidan Letham[13] studied

the influence of gas slippage effect on experimental permeability and discussed the possibility of introducing errors when measuring permeability without considering gas slippage effect. Zhang Hui[7] established a mathematical model of gas well productivity affected by the change of gas-water two-phase permeability. It is considered that the influence of gas well water productivity on the actual productivity of gas well is great and can not be neglected.

For anisotropic fractured gas reservoirs, productivity simulation models mainly include continuum model[14], discrete fracture network model[15], equivalent continuum model[16]. Among them, equivalent continuum model is based on discrete fracture network model, and the effect of fracture is reflected in the increase of permeability and porosity. The equivalent permeability tensor of fractured reservoir rock can be obtained by flow equivalence principle[17]. Li Yajun[18] established a mathematical model for calculating the equivalent permeability tensor of fractured reservoirs, solved it by boundary element method, and proposed a method for determining the Representative Element Volume of fractured reservoirs. Chen S H[19] et al. used Monte Carlo method to generate randomly distributed fractures, and the seepage characteristics of geological model with random fractures were analyzed. The permeability tensors and Representative Element Volume corresponding to different fracture densities, fracture azimuths, and model sizes were calculated.

Based on the equivalent permeability tensor model of fractured media, this paper established a seepage model considering multiple factors such as reservoir stress sensitivity, slippage effect, permeability anisotropy and gas-water two-phase permeability change, deduced the corresponding production equation, and quantitatively analyses the influencing factors of gas-water co-production well productivity, so as to provide theoretical support for water-gas well productivity evaluation and rational allocation of production.

2. Mathematical model

2.1 Stress sensitivity model

The porosity and permeability of fractured reservoir will decrease with the increase of effective stress. Because of the low matrix porosity and permeability in fractured reservoir, the stress sensitivity is mainly caused by natural fractures. Based on Kozeny-Carman equation, Mckee[20], Chen[21] and others deduced a permeability model with effective stress for fractured reservoirs. The permeability is expressed as:

$$K_f = K_{f0} e^{-3C_f(\sigma_e - \sigma_{e0})} \quad (1)$$

2.2 Slippage effect model

When the pressure is very low and the average free path of gas molecule reaches the pore size, the diffusion of gas molecules can move freely without collision. When gas phase flows in reservoir rocks, there is no adsorbed thin layer on the pore wall, and the flow velocity has no obvious difference between the center of the pore and the wall of the pore, which leads to the increase of apparent permeability. Experiments show that the lower the rock permeability, the more obvious the slippage effect, and the lower the pressure, the more obvious the slippage effect[22].

Klinkenberg[23] established the relationship between permeability considering slippage effect and permeability without considering the slippage effect.

$$K_l' = K_l \left(1 + \frac{b_k}{p_g} \right) \quad (2)$$

The b_k defined by Klinkenberg is related to pressure and average molecular free path.

$$\frac{b_k}{p_g} \approx \frac{4\lambda_m}{r} \quad (3)$$

b_k is a coefficient related to K_0 . Heid[24] and others have given the relationship between b_k and K_0 through experiments.

$$b_k = 11.419K_0^{-0.39} \tag{4}$$

2.3 Non-darcy seepage velocity model

Fractured gas reservoir seepage theory is complex, the seepage velocity in the fracture is larger, which obeys the law of high-speed non-linear seepage, while the seepage velocity in the matrix is smaller, which obeys the law of low-speed non-linear seepage.

In the fracture, the permeability under the condition of high-speed non-linear seepage is expressed as[25-26]:

$$K'_f = \frac{\mu}{\frac{\mu}{K_{f0}} + \xi \rho_g v K_r} \tag{5}$$

Where, $\xi = \frac{1}{[\phi(1-S_w)]^2} e^{45 - \sqrt{407 + 81 \times \ln(K_{f0}/(\phi(1-S_w)))}}$

In the matrix, the permeability under the condition of low-velocity non-linear seepage is expressed as[26]:

$$K'_m = \frac{K_{m0} \mu v}{\mu v - K_{m0} K_r \gamma} \tag{6}$$

2.4 Equivalent permeability tensor model

Equivalent permeability tensor of fractured media can express the effect of natural fractures on the permeability of matrix, and can fully characterize heterogeneity and anisotropy of fractured reservoirs. Equivalent permeability tensor K can be expressed as[27]:

$$K = \begin{bmatrix} K_{xx} & K_{xy} \\ K_{yx} & K_{yy} \end{bmatrix} \tag{7}$$

According to Darcy's law, the velocity V and pressure gradient ∇P of a fluid through a homogeneous anisotropic continuum characterized by a permeability tensor can be expressed as:

$$V = -\frac{K}{\mu} \nabla P \tag{8}$$

The component V_x and V_y of the average velocity V at the outer boundary of fractured reservoir are respectively:

$$\begin{cases} V_x = \frac{1}{l_y} \left| \int_{\Gamma_2} V \cdot n_2 dy \right| \\ V_y = \frac{1}{l_x} \left| \int_{\Gamma_3} V \cdot n_3 dx \right| \end{cases} \tag{9}$$

As shown in Figure 1, the rectangular area with size $l_x \times l_y$ includes porous media area Ω_m and fracture area Ω_f nested in the matrix block. The outer boundary of the area Ω is Γ_b ($b=1,2,3,4$). The unit normal vector on the outer boundary is n_b , and the inner boundary is the interface Ω_{mf} between matrix and fracture.

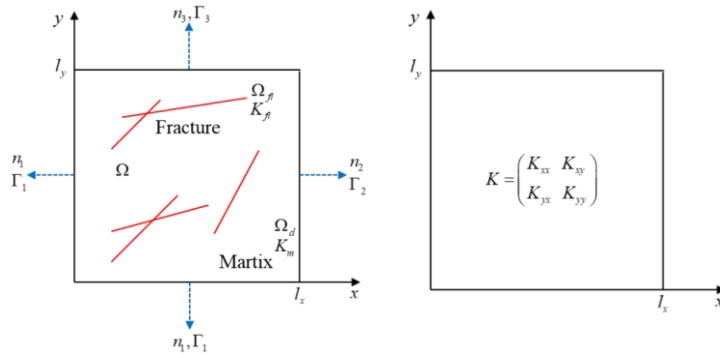


Figure 1 Schematic diagram of equivalent permeability tensor in fractured media

The permeability tensor[18] in the physical sense can be obtained by using periodic boundary conditions. As shown in Figure 1, the periodic boundary conditions of the grid block are expressed as follows:

$$\begin{cases} P_{fi}|_{\Omega_{fmi}} = P_m|_{\Omega_{fmi}} \\ (V_{fi} \cdot n)|_{\Omega_{fmi}} = (V_m \cdot n)|_{\Omega_{fmi}} \\ P|_{y=0} = P|_{y=l_y} - l_y \frac{\partial P}{\partial y} & (\Gamma_1, \Gamma_3) \\ V|_{y=0} \cdot n_1 = -V|_{y=l_y} \cdot n_3 & (\Gamma_1, \Gamma_3) \\ P|_{x=0} = P|_{x=l_x} - l_x \frac{\partial P}{\partial x} & (\Gamma_2, \Gamma_4) \\ V|_{x=0} \cdot n_2 = -V|_{x=l_x} \cdot n_4 & (\Gamma_2, \Gamma_4) \end{cases} \quad (10)$$

Where, Ω_m is the area of fracture i in matrix block.

2.5 Gas-water two phase productivity model

According to the equivalent permeability tensor model, the natural fracture is treated equivalently, and the permeability distribution in the study area is calculated. The gas-water two-phase seepage model[28] is established by neglecting the vertical flow of fluid.

Gas continuity equation:

$$\frac{\partial}{\partial x} \left(\frac{\rho_g K_{xx} K_{rg}}{\mu_g} \frac{\partial p_g}{\partial x} + \frac{\rho_g K_{xy} K_{rg}}{\mu_g} \frac{\partial p_g}{\partial y} \right) + \frac{\partial}{\partial y} \left(\frac{\rho_g K_{yx} K_{rg}}{\mu_g} \frac{\partial p_g}{\partial x} + \frac{\rho_g K_{yy} K_{rg}}{\mu_g} \frac{\partial p_g}{\partial y} \right) = \frac{\partial}{\partial t} (\phi S_g \rho_g) \quad (11)$$

Where, $\rho_g = \frac{PM_g}{ZRT}$

Water continuity equation:

$$\frac{\partial}{\partial x} \left(\frac{\rho_w K_{xx} K_{rw}}{\mu_w} \frac{\partial p_w}{\partial x} + \frac{\rho_w K_{xy} K_{rw}}{\mu_w} \frac{\partial p_w}{\partial y} \right) + \frac{\partial}{\partial y} \left(\frac{\rho_w K_{yx} K_{rw}}{\mu_w} \frac{\partial p_w}{\partial x} + \frac{\rho_w K_{yy} K_{rw}}{\mu_w} \frac{\partial p_w}{\partial y} \right) = \frac{\partial}{\partial t} (\phi S_w \rho_w) \quad (12)$$

The relationship between gas-water saturation and capillary pressure is as follows:

$$\begin{aligned} S_g + S_w &= 1 \\ P_{cwg} &= P_g - P_w \end{aligned} \quad (13)$$

The initial and boundary conditions are:

$$\begin{aligned}
 P|_{t=0} &= P_{gi} \\
 S_w|_{t=0} &= S_{wi} \\
 \left. \frac{\partial P_g}{\partial x} \right|_{x=0, x=l_x} &= 0 \\
 \left. \frac{\partial P_g}{\partial y} \right|_{y=0, y=l_y} &= 0
 \end{aligned} \tag{14}$$

3. Solution method

The equivalent permeability tensor model is solved by boundary element method. The solution steps are as follows: discretizing the research area into finite grids, selecting the *i*-th grid, discretizing the grid boundary and fracture boundary, calculating the correlation coefficient of bedrock and fracture system equation, solving the system equation, calculating the equivalent permeability tensor, and continuing the calculation of the next grid.

The gas-water two-phase seepage model is discretized by the finite difference method, a δp and δS_w are solved by the IMPES method. Then the pressure and water saturation can be obtained. The gas output can be expressed as [29]:

$$Q_g = \frac{d_x H \left(\frac{K_{yx_{i,j\pm 1}}}{dx} + \frac{K_{yy_{i,j\pm 1}}}{dy} \right)}{\mu B} (P_{i,j\pm 1} - P_{wf}) + \frac{d_y H \left(\frac{K_{xy_{i\pm 1,j}}}{dx} + \frac{K_{xx_{i\pm 1,j}}}{dy} \right)}{\mu B} (P_{i\pm 1,j} - P_{wf}) \tag{15}$$

4. Case study

Taking Kuche Piedmont fractured tight gas reservoir in Xinjiang as an example, the basic parameters are shown in Table 1.

Table 1 Basic parameters in the simulation

Initial permeability of natural fracture	0.1D	Initial permeability of hydraulic fracture	200D
Fracture compression coefficient change rate	0.2MPa ⁻¹	Initial compression coefficient of fracture	0.1MPa ⁻¹
Viscosity of natural gas	0.01mP·s	Viscosity of formation water	1mPa·s
Matrix porosity	0.01	Water saturation	0.3
Natural gas density	0.75kg/m ³	Formation water density	1070kg/m ³
Initial permeability of matrix	0.005mD	Air water interfacial tension	0.2mN/m
Formation pressure	65MPa	Starting pressure gradient	0.015MPa/m
Natural fracture opening	Distribution law	Normal distribution	Distribution law
	Mean value	100μm	Natural fracture length
	Standard deviation	32	Mean value
Natural fracture azimuth	Distribution law	Fisher distribution	Standard deviation
	Mean value	20	Reservoir thickness
	K_{fisher}	10	Linear density of natural fracture
		Simulation area width	30m
			1.1/m
			500×500m

There is a 200 m artificial fracture in the study area. The fracture model is shown in Fig.2 and the permeability tensor is shown in Fig.3.

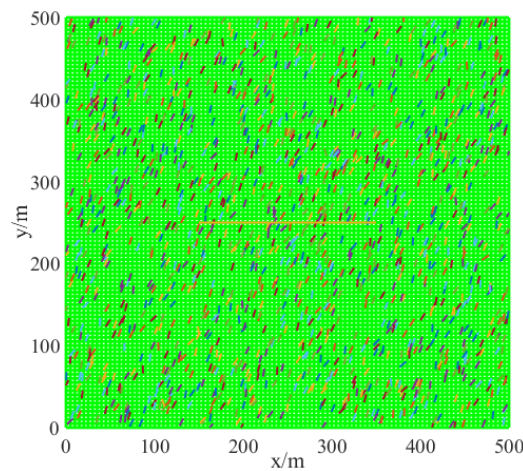


Figure 2 Fracture distribution model

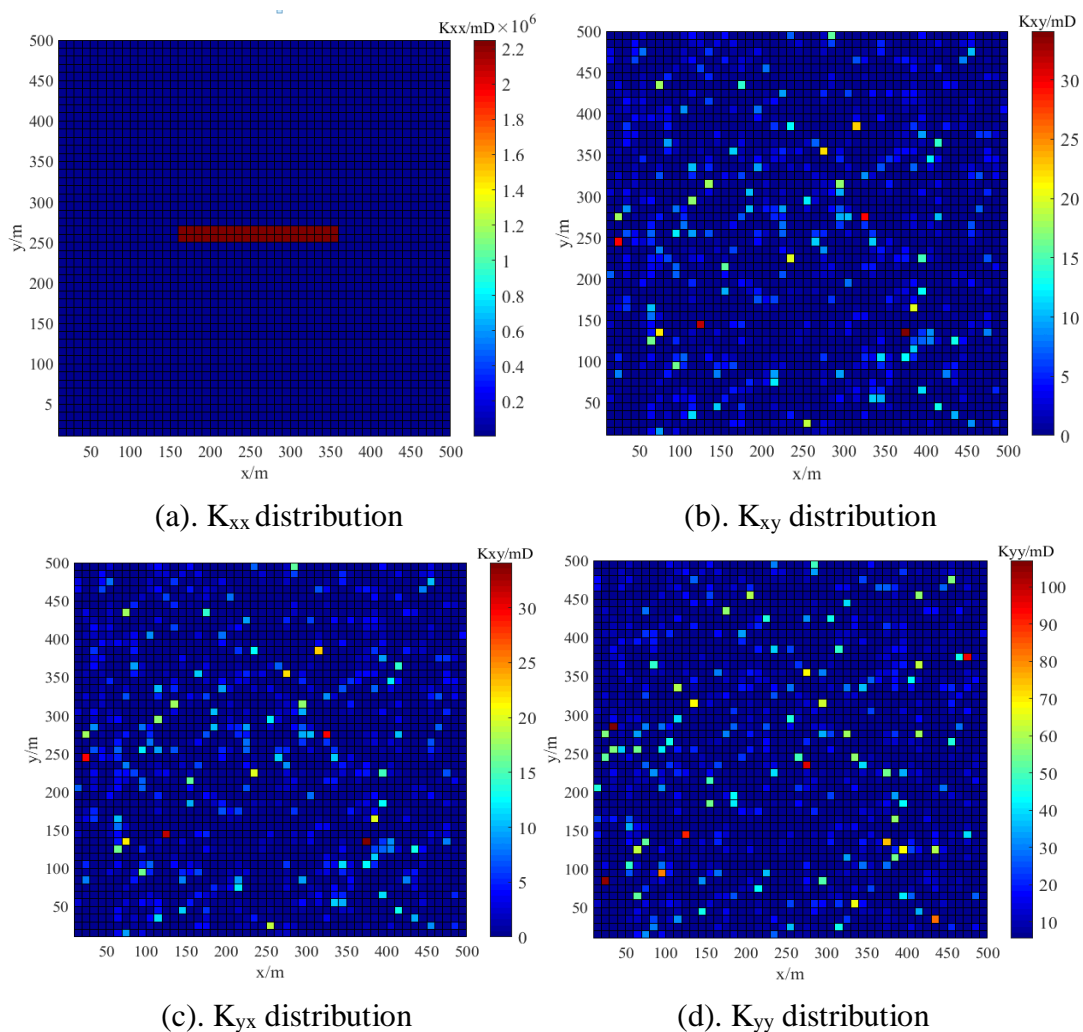


Figure 3 Permeability tensor distribution

According to formula (11), the production curve under different conditions can be calculated (Fig.4 and Fig.5).

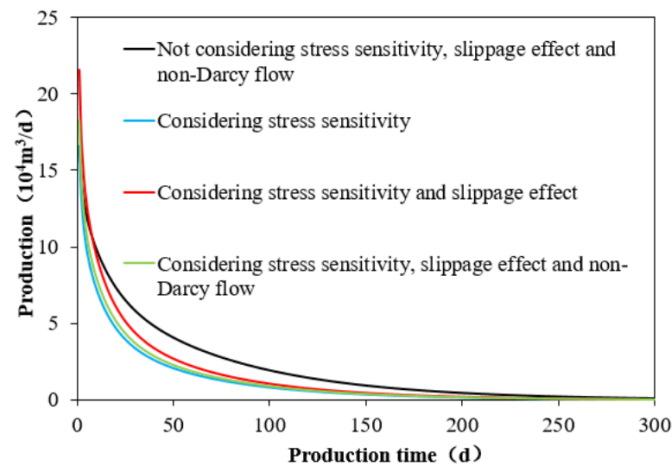


Figure 4 Production curve under different conditions

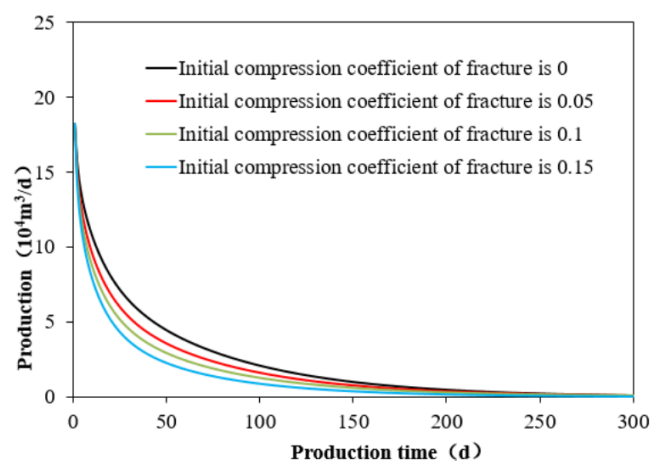


Figure 5 Production curve under different initial fracture compression coefficients

Fig.4 shows that when stress sensitivity, slippage effect, and non-Darcy flow are not taken into account, the calculated production is on the high side. After introducing stress sensitivity, slippage effect and non-Darcy flow, the calculated production decreases, and the production varies with different factors. Therefore, for anisotropic fractured gas reservoirs, the productivity of gas wells will be overestimated without considering the above factors.

Fig.5 shows the production curve under different initial fracture compression coefficients. In the early stage of production, stress sensitivity has little effect on gas production. After a certain period of production, the production decline caused by stress sensitivity gradually increases. When production lasts for about 50 days, stress sensitivity has the greatest impact. At the later stage of production, there is little difference in production under different initial compression coefficients of fractures. The main reason may be that the formation energy is sufficient in the early stage of production and the effective permeability decline is not obvious. In the middle stage of production, the formation energy decreases, the effective stress decreases, and the effective permeability of natural fracture decreases greatly. In the later stage of production, the energy decreases to a lower level, the natural fracture is no longer further closed, and the effective permeability tends to be stable.

Compared with conventional gas reservoirs, fractured gas reservoirs have the following characteristics: (1) reservoir anisotropy, in other words, the permeability difference in different directions is large; (2) the main seepage channel is natural fracture, which is affected by effective stress, natural fracture closure, and effective permeability reduction has a greater impact on productivity. The unsteady gas production equation established in this paper is used to analyze the gas production under different natural fracture densities.

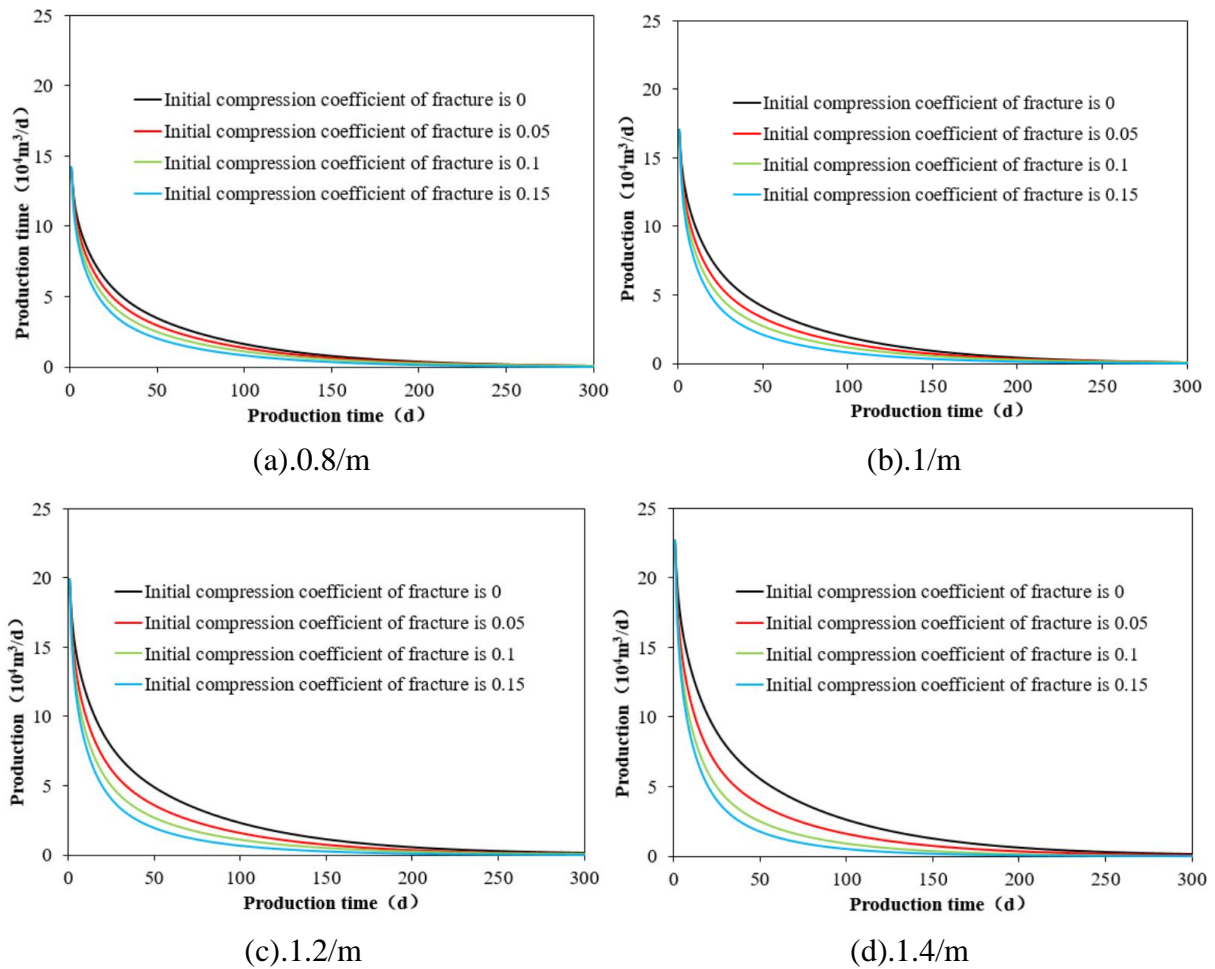


Figure 6 Gas well productivity under different natural fracture densities

Figure 6 shows the production curve under different natural fracture density and initial compression coefficient. When the density of natural fracture is small, the effect of the initial compression coefficient of fracture on production is small. With the increase of natural fracture density, the effect of initial compression coefficient of fracture on production is more and more obvious. This is because when the number of natural fractures is small, slippage effect and non-Darcy flow are the main factors affecting productivity, while stress sensitivity is relatively small. With the increase of natural fracture density, slippage effect and non-Darcy flow have little effect, and the negative effect of effective stress reduction on natural fracture closure is more significant.

5. Conclusions

In this paper, a gas-water two-phase seepage mathematical model considering reservoir stress sensitivity, slippage effect, and non-Darcy seepage is established, and the effect of each factor on the productivity of anisotropic fractured gas reservoirs is quantitatively analyzed with examples.

With the progress of the production process, reservoir pressure decreases gradually, natural fractures tend to close, which has a greater impact on gas well productivity. Slippage effect increases actual permeability, and non-Darcy flow has a certain impact on productivity. When calculating gas well productivity, the three factors can not be ignored. In the early stage of production, the formation energy is sufficient, and the formation pressure drop has little effect on the effective permeability of natural fractures. With the formation energy attenuation, the closure speed of natural fractures is accelerated, and the stress sensitivity phenomenon is more and more obvious. In the later stage of production, the width of natural fractures tends to be stable, and the stress sensitivity phenomenon gradually weakens. The higher the density of natural fractures is, the more obvious the decrease in

production caused by stress sensitivity is. In the production process, attention should be paid to the selection of appropriate production pressure differences to prevent the rapid closure of natural fractures.

Nomenclature

- K_f Fracture permeability considering stress sensitivity, D;
 K_{f0} Initial fracture permeability, D;
 C_f Fracture compression coefficient, MPa⁻¹;
 σ_e Effective stress, MPa;
 σ_{e0} Initial effective stress, MPa;
 C_{f0} Initial compression coefficient of fracture, MPa⁻¹;
 α_f Change rate of fracture compression coefficient relative to effective stress, MPa⁻¹;
 K_l' Permeability considering slippage effect, D;
 K_l Permeability without considering slippage effect, D;
 b_k Slippage coefficient, MPa;
 p_g Gas phase pressure, MPa;
 λ_m Average free path of gas molecule at pressure at p_g , m;
 r Flow channel size, m;
 l Identifier, $l = m, f$, m represents matrix and f represents fracture;
 μ Gas viscosity, mPa·s;
 ξ Coefficient of inertia, dimensionless;
 ρ_g Gas density, kg/m³;
 v Seepage velocity, m/s;
 K_r Relative permeability, dimensionless;
 ϕ Porosity, 0.9 in the fracture;
 S_w Water saturation, dimensionless;
 K_{m0} Initial permeability of matrix, mD;
 γ Starting pressure gradient, MPa/m;
 P Pore pressure, Pa;
 K_m Permeability of matrix block, D;
 K_{fi} Permeability of fracture i, D;
 P_m Pore pressure of matrix block, MPa;
 P_{fi} Fracture pressure at the interface between fracture i and matrix block, MPa;
 q_{im} Volume flow between matrix block and all fractures, m³/s;
 q_{imi} Volume flow between fracture i and matrix block, m³/s;

- S_g Gas saturation, dimensionless;
- P_{cwg} Capillary force, Pa;
- d_x X-direction grid length, m;
- d_y Y-direction grid length, m;
- H Reservoir thickness, m;
- $P_{i,j\pm 1}$ 、 $P_{i\pm 1,j}$ Pressure in adjacent meshes of wellbore, Pa;
- P_{wf} Bottom hole flow pressure, Pa;
- B Gas volume coefficient, dimensionless.

Acknowledgements

This work was supported by the National Natural Science Foundation of China (Grant No. 5197041731), National Science and Technology Major Projects (Grant No. 2016ZX05052, 2016ZX05014) and the Open Funding of State Key Laboratory of Oil and Gas Reservoir Geology and Exploitation (Southwest Petroleum University) (Grant No. PLN1214).

References

- [1] Yao S, Zeng F, Liu H. A semi-analytical model for hydraulically fractured horizontal wells with stress-sensitive conductivities[J]. Environmental Earth Sciences, 2013, 507(1):201-212.
- [2] Xu W, Wang X, Hou X, et al. Transient analysis for fractured gas wells by modified pseudo-functions in stress-sensitive reservoirs[J]. Journal of Natural Gas Science & Engineering, 2016, 35:1129-1138.
- [3] Dou H, Zhang H, Yao S, et al. Measurement and evaluation of the stress sensitivity in tight reservoirs[J]. Petroleum Exploration & Development, 2016, 43(6):1116-1123.
- [4] Chen D, Pan Z, Ye Z, et al. A unified permeability and effective stress relationship for porous and fractured reservoir rocks[J]. Journal of Natural Gas Science & Engineering, 2016, 29:401-412.
- [5] Wang L, Wang X. Modelling of pressure transient behaviour for fractured gas wells under stress-sensitive and slippage effects[J]. International Journal of Oil Gas & Coal Technology, 2016, 11(1):18-38.
- [6] Florence F A, Rushing J, Newsham K E, et al. Improved Permeability Prediction Relations for Low Permeability Sands[J]. Rocky Mountain Oil & Gas Technology Symposium, 2007.
- [7] Zhang H, Wang L, Wang X, et al. Productivity analysis method for gas-water wells in abnormal overpressure gas reservoirs[J]. Petroleum Exploration & Development, 2017, 44(2):280-285.
- [8] WANG Lu, YANG Shenglai, LIU Yicheng, et al. Experiments on gas supply capability of commingled production in a fracture-cavity carbonate gas reservoir[J]. Petroleum Exploration and Development, 2017, 44(5): 779-787.
- [9] Liu Z, Zhao J, Liu H, et al. Experimental Simulation of Gas Seepage Characteristics of a Low-Permeability Volcanic Rock Gas Reservoir Under Different Water Saturations[J]. Chemistry & Technology of Fuels & Oils, 2015, 51(2):199-206.
- [10] Zhao Y L, Zhang L H, Xu B Q, et al. Analytical solution and flow behaviour of horizontal well in stress-sensitive naturally fractured reservoirs[J]. International Journal of Oil Gas & Coal Technology, 2016, 11(4):350-370.
- [11] Yang Y, Zhang W, Gao Y, et al. Influence of stress sensitivity on microscopic pore structure and fluid flow in porous media[J]. Journal of Natural Gas Science & Engineering, 2016, 36:20-31.

- [12] Behrang A, Mohammadmoradi P, Taheri S, et al. A theoretical study on the permeability of tight media; effects of slippage and condensation[J]. Fuel, 2016, 181:610-617.
- [13] Letham E A, Bustin R M. The impact of gas slippage on permeability effective stress laws: Implications for predicting permeability of fine-grained lithologies[J]. International Journal of Coal Geology, 2016, 167:93-102.
- [14] WARREN J E, ROOT P J. The behavior of naturally fractured reservoirs [J]. SPE Journal, 1963, 3(3):245-255.
- [15] HUSSEIN H, ABBAS F. An efficient numerical model for incompressible two-phase flow in fractured media[J]. Advances in Water Resources, 2008, 31(6): 891-905.
- [16] Snow D T. Anisotropic Permeability of Fractured Media[J]. Water Resources Research, 1969, 5(6):1273-1289.
- [17] Dufolsky L J. Numerical calculation of equivalent grid block permeability tensors of heterogeneous porous media : Water Resour Res, V27, N5, May 1991, P299–708[J]. International Journal of Rock Mechanics & Mining Sciences & Geomechanics Abstracts, 1991, 28(6):A350.
- [18] Li Yajun, Yao Jun, Huang Zhaoqin, et al. Calculation of equivalent permeability tensor and characterization of unit volume in fractured reservoirs. [J]., research and progress in hydrodynamics, 2010, 25 (1): 1-7.
- [19] Chen S H, Feng X M, Isam S. Numerical estimation of REV and permeability tensor for fractured rock masses by composite element method[J]. International Journal for Numerical & Analytical Methods in Geomechanics, 2010, 32(12):1459-1477.
- [20] Mckee C R, Bumb A C, Koenig R A. Stress-dependent permeability and porosity of coal[J]. Spe Formation Evaluation, 1988, 3(1):81-91.
- [21] Chen, D., Pan, Z., Ye, Z., 2015. Dependence of gas shale fracture permeability on effective stress and reservoir pressure: model match and insights. Fuel 139,383e392
- [22] Zou J, Chen W, Yang D, et al. The impact of effective stress and gas slippage on coal permeability under cyclic loading[J]. Journal of Natural Gas Science & Engineering, 2016, 31:236-248.
- [23] Klinkenberg L J. The Permeability of Porous Media To Liquids And Gases[J]. Socar Proceedings, 1941, 2(2):200-213.
- [24] Heid J G, McMahon J J, Nielsen R F, et al. Study of the Permeability of Rocks to Homogeneous Fluids[J]. American Journal of Roentgenology, 1950, 139(2):333-4.
- [25] Coats K H, Nielsen R L, Terhune M, et al. Simulation of Three-Dimensional, Two-Phase Flow In Oil and Gas Reservoirs[J]. Society of Petroleum Engineers Journal, 1967, 7(7):377-388.
- [26] Zhou Hongbo. Super double medium simulation model of nonlinear complex seepage flow law [D]. Southwest Petroleum University, 1999.
- [27] Wang Z, Ran B, Tong M, et al. Forecast of fractured horizontal well productivity in dual permeability layers in volcanic gas reservoirs[J]. Petroleum Exploration & Development, 2014, 41(5):642-647.
- [28] Guo Q, Chen N, Xie H, et al. Three-dimensional hydrocarbon migration and accumulation modeling based on finite volume method[J]. Petroleum Exploration & Development, 2015, 42(6):893-903.
- [29] FANG Wenchao, JIANG Hanqiao, LI Junjian, et al. A numerical simulation model for multi-scale flow in tight oil reservoirs[J]. Petroleum Exploration and Development, 2017, 44(3): 415-422.